

### 3D simulation on turbulent heat transfer in a tube fitted with 30° angled orifices

Ratsak Poomsalood, Pongjet Promvonge\* and Nuthvipa Jayranaiwachira

Department of Mechanical Engineering, Faculty of Engineering,  
King Mongkut's Institute of Technology Ladkrabang, Bangkok 10520, Thailand

\*Corresponding Author, E-mail address: kppongje@kmitl.ac.th, Tel 0-2329-8350, Fax 0-2329-8352

#### **Abstract**

Turbulent periodic flow and heat transfer behaviors in a three dimensional circular tube mounted repeatedly with 30° angled orifices are investigated numerically in the present work. The 30° angled orifice characteristics are orifice-height to tube-diameter ratio or blockage ratio, BR = 0.15 and orifice-pitch spacing to tube diameter ratio, PR, in the range of 1.75–2.50 are introduced. The computations are based on a finite volume method with the SIMPLE algorithm for the pressure-velocity coupling. The fluid flow and heat transfer characteristics are presented for Reynolds numbers from 5000 to 20,000. An effect of the pitch length ratio, PR on the heat transfer and friction factor in the tube is examined and the result is also compared with those of the smooth tube. The study shows that the angled orifice provides higher heat transfer rate and friction factor than the smooth tube for all cases. The increase of the PR leads to the decrease in the Nusselt number and friction factor. The maximum thermal performance of about 1.55 is found for PR=1.75 at the lowest Re.

**Keywords:** circular tube, angled orifice, heat transfer, friction factor, turbulent flow.

#### **1. Introduction**

For several decades, turbulators such as ribs fins grooves or baffles have been used in many applied engineering works due to their high thermal loads and decreased dimensions. The cooling or heating fluid is supplied into the tubes/ducts mostly mounted with several ribs/fins to increase the degree of cooling or heating levels and this configuration is often used in the design of heat exchangers. Therefore, the rib spacing length, angle of attack and height are among the most important parameters in the design of tube/duct heat exchangers.

The concept of periodically fully developed flow was first introduced by Patankar et al. [1] to numerically investigate the heat transfer and flow characteristics in a duct/tube. Since then, the periodically fully developed flow condition has been widely used to study thermal characteristics in transverse-ribbed ducts with different rib heights and pitch spacing lengths [2, 3].

A numerical investigation of laminar forced convection in a three-dimensional duct with ribs/baffles for periodically fully developed flow and with a uniform heat-flux was conducted by Lopez et al. [4]. Sripattanapipat and Promvonge [5] numerically studied the laminar periodic flow

## CST-1021

and thermal behaviors in a two dimensional channel fitted with staggered diamond-shaped baffles and found that the diamond baffle with half apex angle of 5–10° performs slightly better than the flat baffle. Promvonge et al. [6] also examined numerically the laminar heat transfer in a square channel with 45° angled baffle placed on one wall and reported that a single streamwise vortex flow occurs and induces impingement jets on the wall of the inter-baffle cavity and the sidewall.

Most of previous investigation works have considered the heat transfer characteristics in a duct with transverse ribs/baffles. Therefore, the turbulent flow study on angled orifices/ribs has rarely been reported in the literature. In the present work, numerical computations for three dimensional turbulent periodic tube flows over the 30° angle ribs/orifices placed periodically on the tube wall are conducted to examine the changes in the flow structure and its thermal performance.

### 2. Mathematical Foundation

The numerical model for fluid flow and heat transfer in a circular tube was developed under the following assumptions: steady, three-dimensional, turbulent, incompressible fluid flow, and constant fluid properties. The body forces, radiation heat transfer and viscous dissipation are ignored. Based on the above assumptions, the tube flow is governed by the continuity, the Navier-Stokes equations and the energy equation. In the Cartesian tensor system these equations can be written as follows:

Continuity equation:

$$\frac{\partial \rho}{\partial t} + \nabla \cdot (\rho \vec{v}) = 0 \quad (1)$$

Momentum equation:

$$\frac{\partial (\rho \vec{v})}{\partial t} + \nabla \cdot (\rho \vec{v} \vec{v}) = \rho g - \nabla p - \nabla \cdot (\bar{\bar{\tau}}) \quad (2)$$

Energy equation:

$$\frac{\partial (\rho E)}{\partial t} + \nabla \cdot (\vec{v} (\rho E + p)) = \nabla \cdot (k_{eff} \nabla T + (\bar{\bar{\tau}}_{eff} \cdot \vec{v})) \quad (3)$$

when

$$\bar{\bar{\tau}} = \mu \left( (\nabla \vec{v} + \nabla \vec{v}^T) - \frac{2}{3} \nabla \cdot \vec{v} I \right)$$

$$E = h - \frac{p}{\rho} + \frac{v^2}{2}$$

Realizable  $k - \mathcal{E}$  equation

$$\frac{\partial (\rho k)}{\partial t} + \frac{\partial}{\partial x_i} (\rho k v_i) = \frac{\partial}{\partial x_j} \left( \alpha_k \mu_{eff} \frac{\partial k}{\partial x_j} \right) + G_k + G_b - \rho \mathcal{E} - Y_M \quad (4)$$

$$\begin{aligned} \frac{\partial (\rho \mathcal{E})}{\partial t} + \frac{\partial}{\partial x_i} (\rho \mathcal{E} v_i) &= \frac{\partial}{\partial x_j} \left( \alpha_{\mathcal{E}} \mu_{eff} \frac{\partial \mathcal{E}}{\partial x_j} \right) + C_{1\mathcal{E}} \frac{\mathcal{E}}{k} (G_k + C_{3\mathcal{E}} G_b) \\ &- C_{2\mathcal{E}} \rho \frac{\mathcal{E}^2}{k} - R_{\mathcal{E}} + S_{\mathcal{E}} \end{aligned} \quad (5)$$

All the governing equations were discretized by the QUICK scheme, pressure-velocity coupling with the SIMPLE algorithm and solved using a finite volume approach [7]. The solutions were considered to be converged when the normalized residual values were less than  $10^{-5}$  for all variables but less than  $10^{-9}$  only for the energy equation.

Four parameters of interest in the present work are the Reynolds number, friction factor, Nusselt number and thermal enhancement factor. The Reynolds number is defined as

$$Re = \rho \bar{u} D / \mu \quad (6)$$

The friction factor,  $f$  is computed by pressure drop,  $\Delta p$  across the length of the periodic tube,  $L$  as

$$f = \frac{(\Delta p / L) D}{\frac{1}{2} \rho \bar{u}^2} \quad (7)$$

The local Nusselt number can be written as

## CST-1021

$$Nu_x = \frac{h_x D}{k} \quad (8)$$

The area-averaged Nusselt number can be obtained by

$$Nu = \frac{1}{A} \int Nu_x \partial A \quad (9)$$

The thermal enhancement factor (TEF)

$$TEF = \frac{h}{h_0} \bigg|_{pp} = \frac{Nu}{Nu_0} \bigg|_{pp} = (Nu/Nu_0)/(f/f_0)^{1/3} \quad (10)$$

where  $Nu_0$  and  $f_0$  stand for Nusselt number and friction factor for the smooth tube, respectively.

### 3. Flow Configuration

#### 3.1 Orifice Geometry and Arrangement

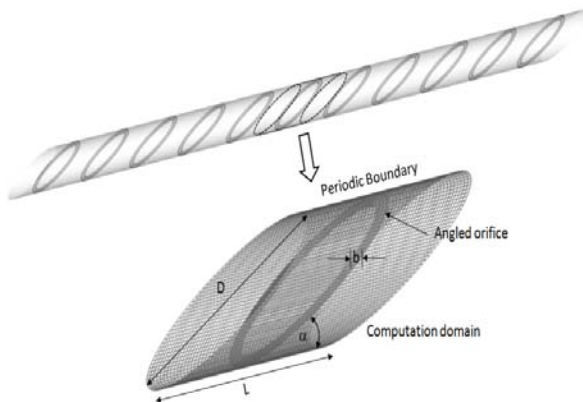


Fig. 1. Tube and computational domain of periodic flow.

The system is a circular tube with multiple 30° angled orifices placed repeatedly in the tube as shown in Fig. 1. The flow under consideration is expected to attain a periodic flow condition in which the velocity field repeats itself from one cell/module to another. The concept of periodically fully developed flow and its solution procedure has been described in Ref. [1]. In the periodic flow module, the air enters the tube at an inlet temperature,  $T_{in}$ , and flows over a 30° angled orifice where  $b$  is the height of the orifice (or the

annulus),  $D$  is set to 0.05 m, is the diameter of tube and  $b/D$  is known as the blockage ratio,  $BR = 0.15$ . The axial pitch,  $L$  or distance between the angled orifice cell is set to  $L = 1.75D$  to  $2.50D$  in which  $L/D$  is defined as the pitch spacing ratio,  $PR = 1.75 - 2.50$ .

#### 3.2 Verification of Smooth Tube

Verification of the heat transfer and friction factor of the smooth-surface tube without orifices is, respectively, performed by comparing with the Dittus–Boelter and Blasius correlations under a similar operating condition as depicted in Fig. 2. The current numerical result is found to be in good agreement with Dittus–Boelter and Blasius correlations obtained from the open literature [8] for both  $Nu$  and  $f$ , less than  $\pm 6.1$  and  $\pm 4.8$  % deviation, respectively.

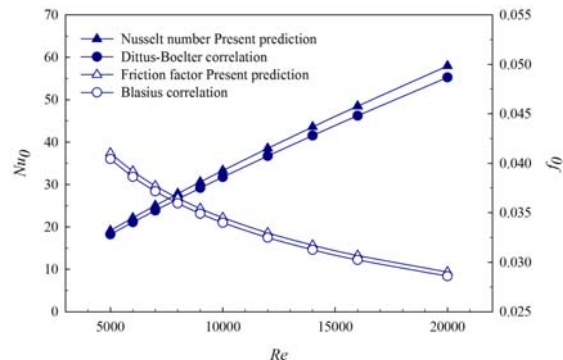


Fig. 2. Verification of  $Nu$  and  $f$  for smooth tube.

#### 3.3 Boundary Conditions

Periodic boundaries are used for the inlet and outlet of the flow domain. Constant mass flow rate of air with 300K ( $Pr = 0.7$ ) is assumed in the flow direction rather than constant pressure drop due to periodic flow conditions. The inlet and outlet profiles for the velocities must be identical. The physical properties of the air have been

## CST-1021

assumed to remain constant at average bulk temperature. Impermeable boundary and no-slip wall conditions have been implemented over the tube wall as well as the orifice. The constant heat flux of the tube wall is maintained at  $600 \text{ W/m}^2$  while the orifice plate is assumed at adiabatic wall conditions.

### 4. Results and Discussion

#### 4.1 Flow Structure

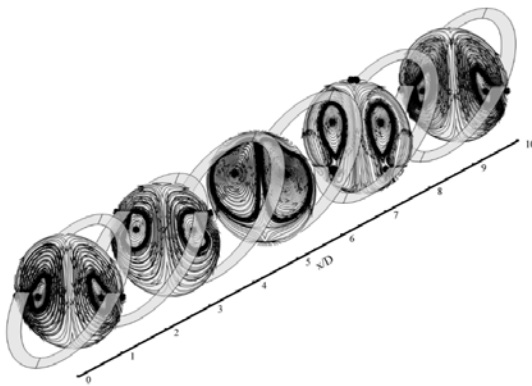


Fig. 3. Streamlines in transverse planes for PR = 1.75 and Re = 12,000.

The flow and vortex coherent structure in the tube fitted with angled orifices can be displayed by considering the streamline plots as depicted in Fig. 3. Here the streamline plot of the angled orifices at Re=12,000, PR=1.75 shows that the presence of orifices can induce the main flow in the tube to become a pair of counter-rotating vortices or common-flow-down vortices. Thus, the impingement/reattachment flow on the lower tube wall is induced, leading to substantial increase in the heat transfer over the tube. The vortex eye/core of both counter-rotating vortex flows moves up from the central area of the left or right half until the flow reaches the next module as can

be seen in Fig. 3. The eye of the vortex repeats itself when it gets to the next cell.

#### 4.2 Heat Transfer and pressure loss

Local  $Nu_x$  contours of the orifice-mounted tube at PR = 1.75 and Re = 12000 are presented in Fig. 4. In the figure, it is apparent that the higher  $Nu_x$  values are seen in a larger area of the tube wall, especially in the bottom region. The peaks are observed at the impingement area on the lower wall where the common-flow-down vortices appear.

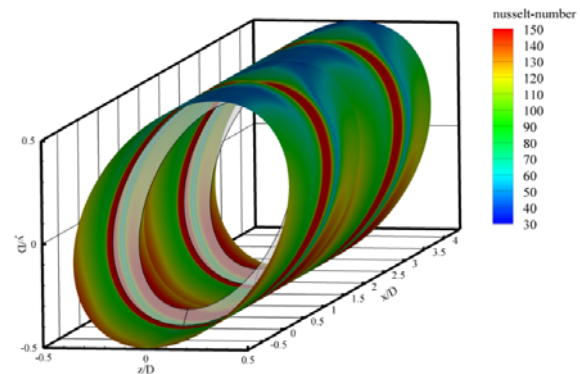


Fig. 4.  $Nu_x$  Contours for PR = 1.75, Re = 12,000.

The variation of the average Nusselt number ratio,  $Nu/Nu_0$ , with Reynolds number at different PR values is depicted in Fig. 5. It is worth noting that the  $Nu/Nu_0$  value tends to decrease with the increment in Reynolds number. The larger PR leads to the decrease in the  $Nu/Nu_0$ . The highest  $Nu/Nu_0$  for the angled orifice at PR = 1.75, BR = 0.15 is found to be about 3.23 times above the smooth tube. The angled orifice in the present work yields the heat transfer rate of about 2.54 – 3.23 times higher than the smooth tube alone.

Figure 6 displays the variation of the friction factor ratio,  $f/f_0$  with Reynolds number for various PRs. It is noted in the figure that the  $f/f_0$  tends to increase with the rise of Reynolds number and the reduction of PR values. The use

## CST-1021

of the angled orifice leads to considerable increase in friction factor in comparison with the smooth tube. The increase in the PR gives rise to the decrease of friction factor. The  $f/f_0$  for the angled orifice is found to be about 7.4–9.1 times depending on the PR and Re values.

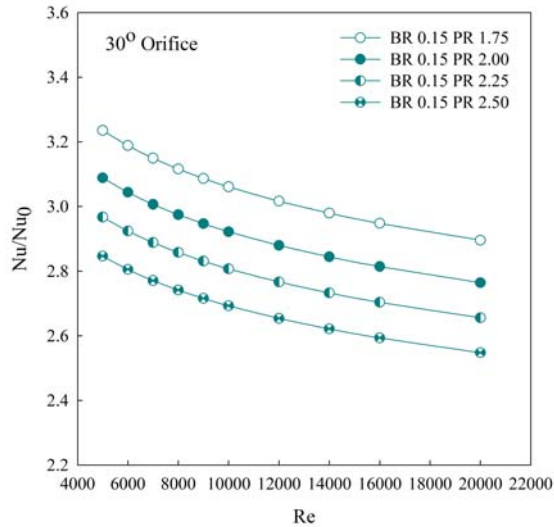


Fig. 5. Variation of  $Nu/Nu_0$  with Re at various PRs.

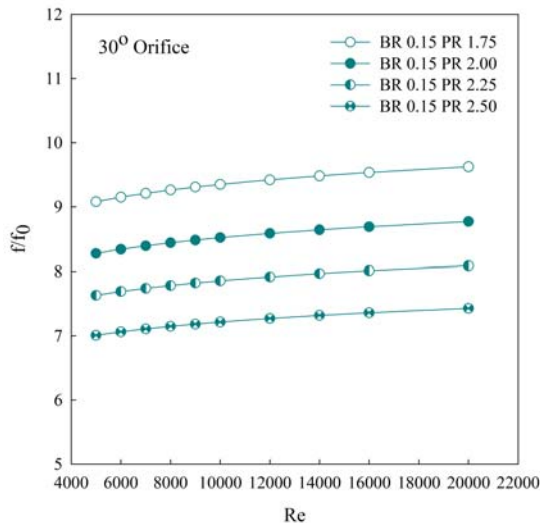


Fig. 6. Variation of  $f/f_0$  with Re at various PRs.

### 4.3 Thermal performance

Figure 7 exhibits the variation of thermal enhancement factor (TEF) with Re for various PR

values. In the figure, the TEF shows a decrease trend with the increment in Re but with the increase in PR values. The TEF values of the angled orifices are varied between 1.30–1.55, depending on the PR and Re values. The maximum TEF is found to be about 1.55 for using the angled orifice at PR = 1.75.

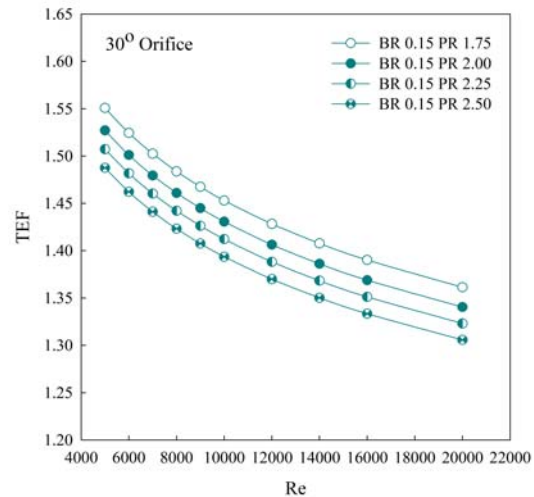


Fig. 7. Effect of PR values on TEF.

## 5. Conclusions

A numerical investigation has been conducted to examine turbulent periodic flow and heat transfer characteristics in a circular tube placed periodically with 30° angled orifices in the tube. Two counter-rotating vortex flows created by the 30° angled orifices exist and help to induce impingement/reattachment flows on the lower tube wall leading to drastic increase in heat transfer rate in the tube. The order of enhancement is about 2.54 – 3.23 times above the smooth tube for the angled orifice at BR=0.15 and PR=1.75–2.50. However, the heat transfer augmentation is associated with enlarged friction loss ranging from 7.42 to 9.08 times above the smooth tube. The highest thermal enhancement

## CST-1021

factor of about 1.55 is found for the angled orifice

### 6. References

[1] Patankar S.V, Liu C.H. and Sparrow E.M. (1977). Fully Developed Flow and Heat Transfer in Ducts Having Streamwise-Periodic Variations of Cross-Sectional Area, *ASME Journal of Heat Transfer.*, vol.99(2), May 1977, pp. 180–186.

[2] Webb B.W. and Ramadhani S. (1985) Conjugate heat transfer in a channel with staggered ribs *International Journal of Heat and Mass Transfer.*, vol.28(9), September 1985, pp. 1679–1687.

[3] Kelkar K.M. and Patankar S.V. (1987). Numerical Prediction of Flow and Heat Transfer in a Parallel Plate Channel With Staggered Fins, *ASME Journal of Heat Transfer.*, vol.109(1), February 1987, pp. 25–30.

[4] Lopez J.R., Anand N.K. and Fletcher L.S. (1996). Heat transfer in a 3-dimensional channel

at  $PR = 1.75$ .

with baffles, *Numerical Heat Transfer. Part A, Applications.*, vol.30(2), 1996, pp. 189–205.

[5] Sripattanapipat S. and Promvong P. (2009). Numerical analysis of laminar heat transfer in a channel with diamond-shaped baffles, *International Communications Heat and Mass Transfer.*, vol.36(1), 2009, pp. 32–38.

[6] Promvong P., Sripattanapipat S., Tamna S., Kwankaomeng S. and Thianpong C. (2010). Numerical investigation of laminar heat transfer in a square channel with 45° inclined baffles, *International Communications Heat and Mass Transfer.*, vol.37(2), 2010, pp. 170–177.

[7] Patankar S.V. (1980). *Numerical heat transfer and fluid flow*. McGraw-Hill. ISBN: 0-07-048740-5 New York. 1980.

[8] Incropera F. and Dewitt P.D, (2006). *Introduction to heat transfer* 5<sup>rd</sup> edition, John Wiley & Sons Inc. 2006